Nonlinear optical properties and surface-plasmon enhanced optical limiting in Ag–Cu nanoclusters co-doped in SiO_2 Sol-Gel films

P. Prem Kiran, B. N. Shivakiran Bhaktha, and D. Narayana Rao[a)]
School of Physics, University of Hyderabad, Hyderabad - 500 046, India

Goutam De
Sol-Gel Division, Central Glass and Ceramic Research Institute, Jadavpur, Kolkata 700 032, India

(Received 11 February 2004; accepted 16 August 2004)

The nonlinear optical properties and the role of the surface-plasmon resonance (SPR) on optical limiting (OL) properties of Ag–Cu nanoclusters co-doped in SiO_2 matrix prepared using the sol-gel technique with a Cu/Ag molar ratio of 1, 2 and 3, respectively, are presented. The studies were made using the second harmonic of high-power nanosecond and picosecond Nd:YAG lasers. These films show a self-defocusing nonlinearity with both nanosecond and picosecond pulses and a good nonlinear absorption behavior with the nanosecond pulse excitation. The nonlinear refractive index decreased with decreasing particle size, whereas the nonlinear absorption increased with an increase in Cu concentration. The observed nonlinear absorption is explained by taking into account the cumulative effect of both the intraband and interband mechanisms. The excitation near the SPR of Cu resulted in an enhanced OL behavior with increasing Cu concentration. No such concentration dependence is observed when the excitation is near the SPR of Ag, however, the limiting threshold is reduced approximately 10–17 times. Excitation at wavelengths far below the SPR of Ag and Cu has not shown any OL behavior. The major contribution toward OL is observed to be from the interband absorption and from a possible energy transfer within the higher unoccupied states of Cu and Ag. Although nonlinear scattering is observed at higher intensities, its contribution is found to be much less than that of the nonlinear absorption assisted by an energy transfer. © *2004 American Institute of Physics*. [DOI: 10.1063/1.1804228]

I. INTRODUCTION

The optical nonlinearity of metal nanoparticles in dielectrics has attracted much attention because of the high polarizability and ultrafast nonlinear response that can be utilized in potential optical devices.[1] Metal clusters and nanoparticles are promising materials for different nonlinear optical (NLO) processes like optical limiting (OL),[2] optical switching, and computing.[3–7] Optical limiters are devices required to protect the sensors and eyes from laser sources by keeping the transmitted energies below the damage threshold.[8] This is achieved with the help of one or more NLO phenomena.[9] Silver,[10] copper,[11] and alloy nanoclusters[12] in semicontinuous thin films, in colloids, and in different glass matrices are extensively studied for the NLO and OL applications.[13–15] Different metal alloy nanoclusters[12,16] are also studied in this aspect. Among the recent challenges are the preparation and characterization of the well-defined nanoscale particles for nonlinear optical evaluations. Different techniques have been developed for promoting the formation of small metal clusters in various matrices. The sol-gel technique of preparing different metal particles in a desired glass matrix is one of them.[17] Different metal particles, organic nanocrystals,[18] fullerenes, and nanoparticles doped in sol-gel glasses[19–21] are well studied for the NLO and OL applications. In this paper, we report the NLO properties and the role of the surface-plasmon resonance (SPR) toward the OL properties of Ag–Cu nanoclusters co-doped in SiO_2 matrix.

II. MATERIAL DESCRIPTION

The composite materials formed by Ag and Cu nanoclusters embedded in a silica glass matrix are prepared by sol-gel technique. A constant $(1Ag+xCu)/SiO_2$ molar ratio of 0.175 is maintained while preparing the films. The samples having the Cu/Ag molar composition of $(x=1)$ 1,2,3 are named as 1Ag1Cu, 1Ag2Cu, and 1Ag3Cu, respectively. All the films show a reasonably homogenous distribution of clusters throughout, and the Cu/Ag atomic ratios are well maintained. The thickness of all the three films used is 150 ± 10 nm. The synthesis and properties of the films used in this study are reported elsewhere.[22] The properties relevant for the present study such as, the size and the shape of the nanoclusters in Ag–Cu films and the linear transmittance at 532 and 435 nm, are given in Table I. The

TABLE I. Size and shape of the nanoclusters in Ag–Cu films studied. Linear transmittance at 532 and 435 nm is given.

Molar ratio	Size		Linear transmittance (%)	
Ag:Cu	(nm)	Shape	532 nm	435 nm
1:1	40–50	Spheroid	77.5	58.5
1:2	25–35	Spheroid and spherical	75	49.5
1:3	15–20	Spherical	72	47.2

[a)]Author to whom correspondence should be addressed; electronic mail: dnrsp@uohyd.ernet.in

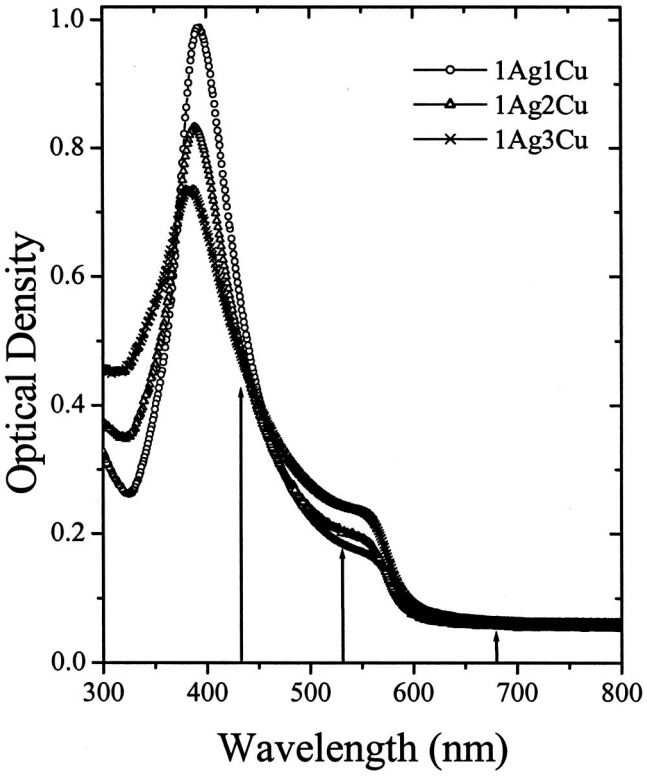

FIG. 1. Absorption spectrum of Ag–Cu nanoclusters co-doped in SiO_2 sol-gel matrix. The arrows indicate the excitation wavelengths used to perform the OL studies.

absorption spectra of the films are shown in Fig. 1, and the arrows indicate the excitation wavelengths used for the OL studies. The films were reheated at 600 °C for 1 h in an 8% of H_2-92% of N_2 atmosphere to remove any oxidation of silver and copper metals embedded in the film. No noticeable change in the absorption spectra is observed before and after the heat treatment. The atomic force microscope images revealed that the films exhibit the same surface characteristics as that of Ref. 22 and the films did not deteriorate with time. The surface-plasmon band, which arises from the oscillations of the free electrons in the conduction band, occupying energy states near the Fermi level, is shifted in these samples compared to that of the pure Ag and Cu nanoclusters embedded in SiO_2. The SPR bands corresponding to both Ag and Cu are clearly seen in the Ag–Cu co-doped films, indicating that these nanoclusters do not form alloys and retain their individuality. In the case of an alloy formation, a single SPR should come between the position of the surface-plasmon band of Ag and Cu, as reported for the Au–Cu (Ref. 1) and Au–Ag (Ref. 23) systems. In the transmission electron microscopy electron diffraction studies, we observed both spots corresponding to Ag and Cu fcc phases, indicating the presence of Ag- and Cu-mixed nanocrystals. The size and distribution of the clusters is clearly dependent on the composition of the film. A distribution of clusters of 5 and 40–50 nm in diameter coexists in the 1Ag1Cu films. With the increasing concentration of copper, the clusters became more spherical. In the 1Ag2Cu film, the relatively larger clusters are spheroid. In the case of the 1Ag3Cu sample, a homogenous distribution of the spherical-shaped clusters with a 5–20 nm diameter is observed. With the increasing concentration of Cu, the distribution of clusters is more uniform. Although in the dipole approximation SPR is independent of the particle size, it has been found that the width and peak position of the SPR band depends on the particle size, shape, and on the environment.[24]

III. EXPERIMENTAL DETAILS

Two frequency-doubled Nd:YAG lasers (532 nm), one with a 6 ns, 10 Hz, repetition rate and another with a 25 ps, 10 Hz repetition rate are used for the experiment. Open and closed aperture *Z*-scan[25] studies are done by focusing the 6 ns laser pulses on to the sample, using a lens of an 80 mm focal length with a beam waist of 30–35 μm at focus, leading to peak intensities in the range of 0.3–1.2 GW cm^{-2}. The transmitted output is collected effectively onto a fast photodiode, which is connected to the data acquisition system consisting of the boxcar averager and computer. Same results are observed with the repeated measurements at different positions on the sample. The open and closed aperture *Z*-scan measurements are used to evaluate the nonlinear absorption and nonlinear refraction properties, respectively. The closed aperture *Z*-scan measurements are also done with the 25 ps pulses, 10 Hz repetition rate to find the contribution of thermal nonlinearities.

Three different excitation wavelengths are used to study the contribution of the SPR band for OL. The 6 ns frequency-doubled Nd:YAG laser (532 nm) generates the first Stokes line at 683 nm (14642 cm^{-1}) and the first anti-Stokes at 435 nm (22952 cm^{-1}), using a Raman cell filled with H_2 gas (vibration mode 4155 cm^{-1}). These Stokes and anti-Stokes lines are used as the excitation wavelengths. The pump, the Stokes, and the anti-Stokes lines are separated by means of a Pellin-Broca prism mounted on a rotation stage. The OL studies are performed using the f/30 geometry for the excitation at 532 nm and the f/15 geometry for the excitations at 435 and 683 nm. The intensity-dependent scattering measurements are done at different angles (θ) from the axis of propagation and at different excitation wavelengths using the 6 ns laser.

IV. RESULTS AND DISCUSSION

A. Nonlinear optical properties

Figures 2(a) and 2(b) show the closed and open aperture transmittance of the *Z*-scan curves, respectively, for the 1Ag2Cu sol-gel film with 6 ns pulses at 532 nm. Figure 3 shows the closed aperture *Z*-scan curve with 25 ps pulses for the 1Ag2Cu sol-gel film at 532 nm. The beam waist at focus of 6 ns and 25 ps pulses is approximately 30 and 35 μm, respectively. The peak intensity at focus for the *Z*-scan measurements for all the films is 0.50 GW cm^{-2} for both the 6 ns and 25 ps pulses. The standard procedure[25] is followed to obtain the pure refractive nonlinearity. The linear absorbance for 1Ag1Cu, 1Ag2Cu, and 1Ag3Cu films at 532 nm is 0.225, 0.25, and 0.28, respectively. The peak-valley trace in the closed aperture *Z* scan shows that these films have self-defocusing (negative, $n_2 < 0$) nonlinearity. Earlier reports on individual Cu and Ag nanoclusters of sizes in the range of

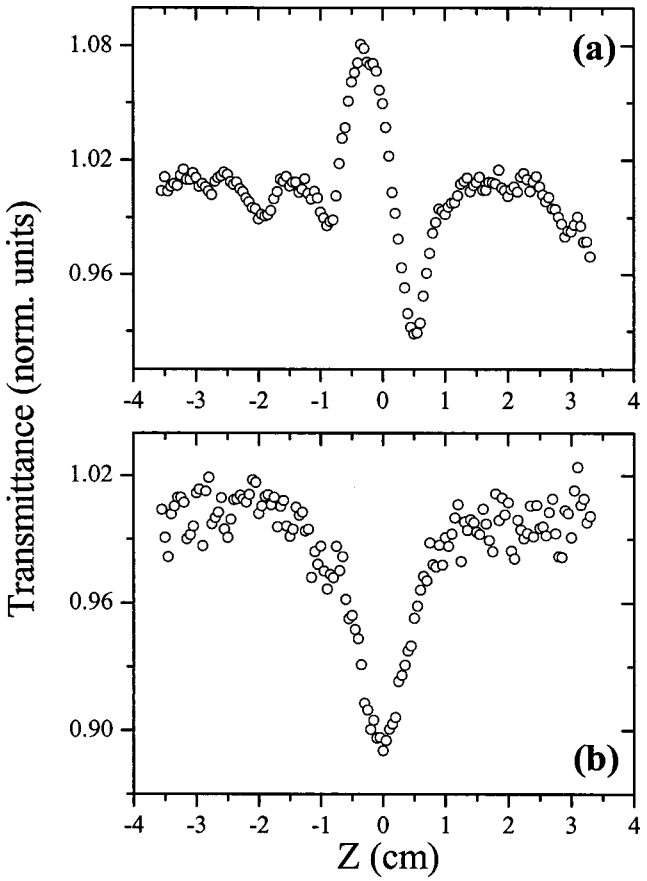

FIG. 2. (a) Closed and (b) open aperture *Z*-scan curves of 1Ag2Cu sol-gel film with 532 nm, 6 ns pulses at an input intensity of 0.32 GW cm^{-2}.

3–10 nm, with picosecond-pulsed lasers[6,26,27] have shown a positive nonlinearity. Whereas, in our case of Ag–Cu composite films, the cluster size varies from 15 to 50 nm, and the contribution will be from both the Ag and Cu nanoparticles. The observed negative nonlinearity could be due to the nonradiative relaxations during the intraband transitions. Although the laser-induced permanent sign reversal of the nonlinear refractive index is reported in Ag nanoclusters in a soda-lime glass,[28] we have not observed any such permanent effect in the intensity ranges used. We observed a good nonlinear absorption with the nanosecond pulse excitation, which increases with the increasing input intensity, whereas no nonlinear absorption is observed on the excitation with picosecond pulses. The nonlinear refractive index n_2 is calculated from the difference between the normalized peak and valley transmittance (ΔT_{p-v}) in the closed aperture *Z* scan using the Eqs. (1)–(4).

$$\Delta T_{p-v} = 0.406(1-S)^{0.25}|\Delta\Phi_0|, \tag{1}$$

$$|\Delta\Phi_0| = (2\pi/\lambda)\gamma I_0 L_{\text{eff}}, \tag{2}$$

$$L_{\text{eff}} = [1-\exp(-\alpha L)]/\alpha, \tag{3}$$

$$n_2(\text{esu}) = (cn_0/40\pi)\gamma(\text{m}^2/\text{W}), \tag{4}$$

where L is the thickness of the sample, α is the linear absorption coefficient at 532 nm, c (m/s) is the speed of light in vacuum, and S is the linear transmittance of the aperture.

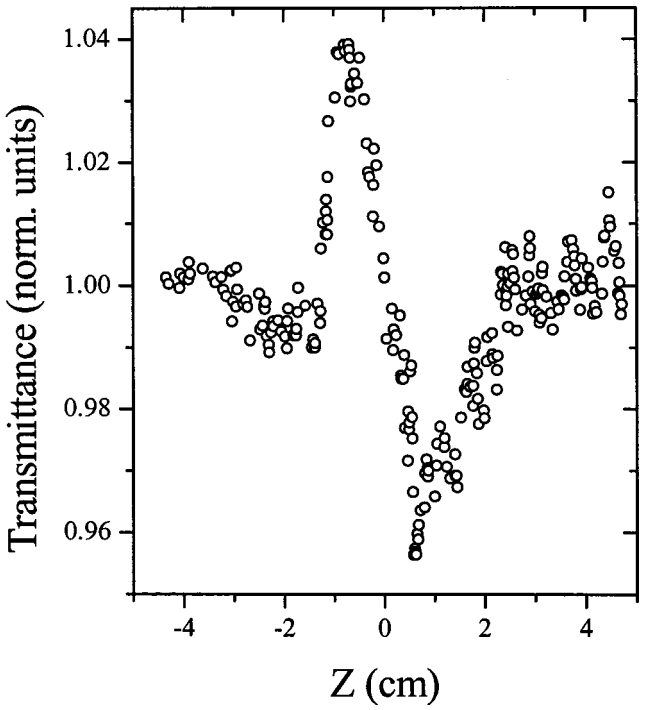

FIG. 3. Closed aperture *Z*-scan curve of 1Ag2Cu sol-gel film with 25 ps pulses at 532 nm.

The nonlinear refractive index n_2 is defined in terms of the ordinary linear index n_0. And the real part of the complex third-order nonlinear dielectric susceptibility $\chi_r^{(3)}$ is defined in Gaussian units by[29]

$$n = n_0 + n_2 I, \qquad n_2(\text{cm}^2\ \text{W}^{-1}) = \frac{0.0395}{n_0^2}\chi_{\text{r}}^{(3)}(\text{esu}), \tag{5}$$

where I is the laser intensity. The estimated values of n_2 and $\chi_r^{(3)}$ for different films with nanosecond and picosecond pulses are given in Table II. For a fixed value of S, with an increasing input intensity, the value of ΔT_{p-v} increases with a dominating valley in the closed aperture *Z*-scan curve, indicating the presence of a nonlinear absorption in these films. The values of the n_2 measured for $\Delta T_{p-v} \sim 15\%$ are of the order of 10^{-9} cm^2/W for all the three films. The closed aperture *Z*-scan curves with the undoped silica film shows a transmission variation $\Delta T_{p-v} < 1.5\%-2\%$, whereas for the doped glass samples, the variation is $>15-20\pm2\%$, which increases with an increasing laser intensity. Table II also gives the normalized transmittance at focus ($T_{z=0}$) and the

TABLE II. Measured values of nonlinear refraction at 532 nm from the closed aperture *Z* scan and normalized transmittance from the open aperture *Z* scan at focus with peak intensities.

	$n_2(\times10^{-9}$ $cm^2/W)$		$\chi_{\text{r}}^{(3)}(\times10^{-7}$ esu)		$T_{Z=0}, I_{00}$
Sample	6 ns	25 ps	6 ns	25 ps	(GW cm^{-2})
1Ag1Cu	3.08±0.4	3.12±0.6	1.65±0.21	1.68±0.43	0.86, 1.14
1Ag2Cu	2.14±0.2	2.90±0.5	1.15±0.12	1.56±0.37	0.83, 0.93
1Ag3Cu	1.66±0.3	2.80±0.5	0.89±0.16	1.50±0.35	0.88, 0.72

peak intensities at the focus I_{00} for the open aperture Z-scan curves. The values of the nonlinear refractive index, n_0, measured with 6 ns and 25 ps pulses at 10 Hz repetition rate are nearly the same. Further, both the nanosecond and picosecond measurements show a decrease in the value of n_2 while going from a film with a low absorbance of 0.225 (1Ag1Cu) to a film of a high absorbance of 0.28 (1Ag3Cu). This result clearly shows that the nonlinearity n_2 is predominantly electronic in origin rather than thermal. If the thermal contributions were dominant, we would see an increase in n_2 with an increase in absorption.

The n_2 values measured with 25 ps pulses show slightly higher values than with the 6 ns pulses. We, however, cannot draw any conclusion from this due to the large pulse-to-pulse fluctuation and the small differences between the nanosecond and picosecond values. These values, however, match with the earlier measurements with the 6 ps, 15.2 MHz repetition rate pulse.[22] The thermal loading effects were reported only at the high repetition rate of 76 MHz, leading to an increase in the nonlinearity by an order of magnitude.[22,30] The figure of merit for the third-order nonlinearity $\chi_r^{(3)}/\alpha$, measured using the two-beam degenerate four-wave mixing configuration by Uchida *et al.*,[15] shows an increase in the value, with the particle size of Cu as well as Ag, with a ratio of 1.7 from 40 to 15 nm Cu particles. Our values measured from the closed aperture Z scan match well with their data for the nanosecond pulses, but give a ratio of 1.1 for the picosecond pulses. We, therefore, attribute the steady increase in the n_2 values to the increase of $\chi_r^{(3)}$ as a function of the particle size from 1Ag3Cu to 1Ag1Cu.

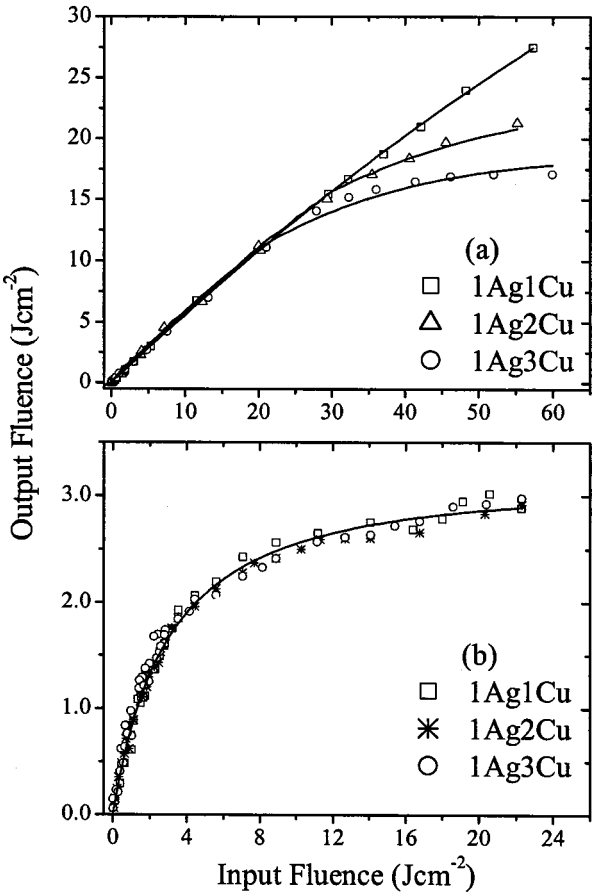

FIG. 4. Optical limiting curves of Ag–Cu metal nanoclusters in sol-gel matrix (a) at 532 and (b) 435 nm. The solid lines are the theoretical fits to the curves.

B. Optical limiting properties

These films are studied for OL, where the input fluence is varied from 30 μJ cm^{-2} to 60 Jcm^{-2}, for the 532 nm excitation, and from 10 μJ cm^{-2} to 23 J cm^{-2} for λ_{ex} ~435 nm excitation. The limiting curves at 532 and 435 nm for these films are shown in Figs. 4(a) and 4(b), respectively. The solid line(s) in Figs. 4(a) and 4(b) show the theoretical fits using Eq. (8). At 532 nm, the limiting threshold has decreased with the increasing Cu/Ag ratio from 47.22 to 27.88 J cm^{-2}, whereas no such concentration dependence is observed with the 435 nm excitation. However, the limiting threshold was reduced to ~2.74 J cm^{-2} in the case of excitation at 435 nm. The excitation at 683 nm has not shown any OL behavior in these films. The limiting threshold ($I_{1/2}$) values are given in Table III.

Different processes like transient absorption, photoejection of electrons by a two-photon or multiphoton absorption,[31] interband and intraband transitions,[13] and nonlinear scattering[32] are reported to be leading to the OL in nanoclusters. A laser pulse can cause an interband or an intraband absorption in the metal nanoparticle system, depending on the excitation wavelength and incident intensity. In the case of Cu, the SPR is situated near the interband transitions $d \rightarrow p$ (E_{dp}=2.17 eV or 571 nm) from the filled d band to the unoccupied states in the p conduction band. For Ag, the SPR is situated well below the interband transition thresholds $d \rightarrow p$ (E_{dp}=3.99 eV or 310 nm) and $p \rightarrow s$ (E_{ps} =3.85 eV or 322 nm) from the occupied p states to the unoccupied s states. When excited at 532 nm (2.33 eV) and 435 nm (2.86 eV), the electrons in the filled d band of Cu will get excited to the unoccupied states in the p conduction band due to the interband transitions. These excited electrons are free carriers attaining a whole spectrum of energies, both kinetic and potential, immediately after the absorption, leading to the bleaching of the ground-state plasmon band. This process is accompanied by the nascent excited state showing a transient absorption due to the free-carrier absorption.[12]

In the case of metal nanoparticles, electron dynamics also play an important role in the interband/intraband transitions, and the possible processes are depicted in Fig. 5. The electron dynamics in metals occur in several steps. One is the nonthermal distribution created by an optical pulse, which

TABLE III. Limiting thresholds and the interband transition coefficients for Ag–Cu films at 532 and 435 nm.

Molar ratio	Limiting threshold, $I_{1/2}$(J cm^{-2})		β_2/n''(cm^2/J)[a]	
Ag:Cu	532 nm	435 nm	532 nm[b]	435 nm[b]
1:1	48.2	2.74	0.00775	0.518
1:2	35.5	2.7	0.01114	0.520
1:3	27.88	2.7	0.01388	0.521

[a] β_2/n'' is the effective nonlinear absorption coefficient.
[b] $1+(2n''/b)$ ~1.575 and 1.113 for 532 and 435 nm.

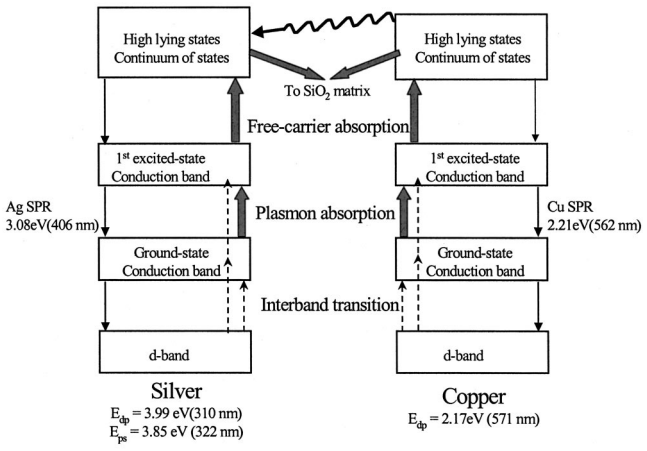

FIG. 5. Energy-level diagram explaining the processes leading to optical limiting in the co-doped Ag–Cu nanoclusters systems. The plasmon absorption and free-carrier absorption (solid block arrows pointing upwards) dominates over the interband transition and two-photon absorption (dotted arrows).

thermalizes to a hot Fermi distribution in the order of few hundreds of femtoseconds. Another is the electron-phonon coupling, which leads to an equilibrium of the electron and lattice temperatures; this takes place and relaxes within a few picosecond time scale.[33,34] The relaxation dynamics of the metal nanoclusters depend on the energy absorbed by the nanoparticles, the size of the nanoparticles, the surrounding matrix, and the excitation wavelength.[35] The relaxation time decreases with a particle diameter at higher energies and is reported to show an increase at the SPR. Faster relaxations make further excitation of the relaxed electrons and further transfer of energy via electron-electron and electron-phonon interaction possible, as the excitation 6 ns laser pulse is present over much wider time scales compared to the relaxation times. The interband transitions between Cu and Ag occur at much slower time scales compared to the intraband transitions, and long-lived free carriers are assumed here to play an important role in the reduction of optical limiting threshold with different Cu–Ag composites.

At 532 nm, as the excitation energy is just above the SPR band and higher than the interband threshold of Cu, it leads to the generation of more free carriers with an increasing Cu concentration. These excited carriers can relax within the Cu energy levels (within a few picoseconds) and can also relax to the conduction band or SPR band of Ag via electron-electron interaction and energy transfer among the higher unoccupied states of these metal nanoclusters, which overlap. Such an exchange process leads to a further bleaching of the Cu surface-plasmon band, which, in turn, will lead to more absorption of the incident laser radiation. The possible processes are shown in Fig. 5 and form the basis for simulating the theoretical curves for the evaluation of a nonlinear attenuation coefficient leading to OL. The solid block arrows pointing upwards show the strong SPR absorption and free-carrier absorption; and the dotted lines show a weak interband and a two-photon absorption.

The extinction coefficient for an ensemble of metal nanoparticles dispersed in a dielectric matrix, can be expressed in terms of the complex dielectric function of the metal nanoparticles $\varepsilon(\omega)=\varepsilon_1(\omega)+i\varepsilon_2(\omega)$ as

$$\kappa=\frac{9V\varepsilon_d^{3/2}}{c}\frac{\omega\varepsilon_2(\omega)}{[\varepsilon_1(\omega)+2\varepsilon_d]^2+\varepsilon_2^2(\omega)}, \tag{6}$$

where ε_d is the dielectric constant of the surrounding matrix and will be assumed frequency independent and real. The absorption is resonantly enhanced close to the SPR frequency, minimizing the denominator, which is the condition for the surface-plasmon resonance.[1] Assuming $\varepsilon(\omega)=n^2(\omega)=[n'(\omega)+in''(\omega)]^2$ and the real part of the linear refractive index, $n'(\omega)$, to be independent of the increasing intensity, whereas the imaginary part, $n''(\omega)$, referred as the attenuation index, changes with the incident intensity. Following the model for OL by Qu *et al.*,[13] the modified extinction coefficient and output transmission after the films can be given as

$$\kappa\approx a\frac{1+\dfrac{\beta_2}{n''}I}{1-\dfrac{2\beta_2}{b}I}, \tag{7}$$

$$I_{\text{out}}=I_{\text{in}}\times T_0\left(\frac{1+\dfrac{\beta_2}{n''}I_{\text{out}}}{1+\dfrac{\beta_2}{n''}I_{\text{in}}}\right)^{1+(2n''/b)}, \tag{8}$$

where $T_0=e^{\kappa_0 L}$ is the linear transmittance of the films and $\beta_2 I$, describing the nonlinear attenuation performance, is comparable with the nonlinear attenuation index n'' for the strong nonlinear absorption. Here, the term β_2/n'' is the effective nonlinear absorption coefficient and it includes the contribution from all the transitions that come into play at the intensities used, i.e., both the interband and intraband transitions, which, in turn, get enhanced because of the energy transfer among the high-lying states from Cu to Ag nanoclusters. Since the excitation wavelengths used are either in resonance or above the surface-plasmon levels, the major contribution will be from the intraband transitions. Using Eq. (8), the OL curves are fitted and the term β_2/n'' explaining the nonlinear absorption is evaluated.

At 435 nm, the SPR of both Cu and Ag will contribute to the nonlinear absorption because the excitation energy is above the SPR of Cu and nearer to the SPR of Ag. The contribution of the SPR bands of both the Ag and Cu nanoclusters toward the nonlinear absorption could be the reason for a drastic reduction in the limiting threshold at 435 nm. It becomes difficult to exactly calculate the contribution of the individual metal nanoclusters, which is also supported by the fact that there is no variation in the limiting threshold with an increasing Cu concentration at this excitation energy. The values representing the nonlinear absorption performance evaluated are given in Table III.

In addition to the processes mentioned earlier, we have also observed the nonlinear scattering at high energies (>10 J cm^{-2}) from these films, which can be seen in the far

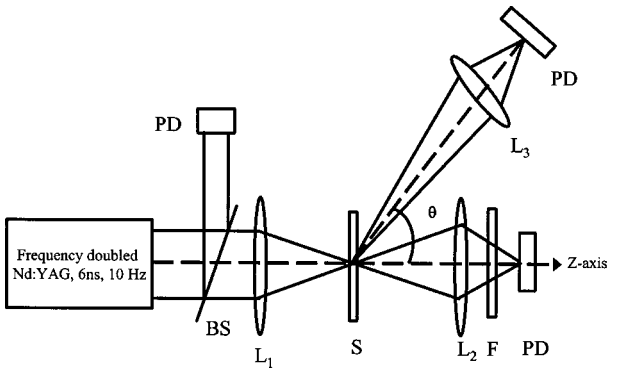

FIG. 6. Nonlinear transmittance and nonlinear scattering setup: L_1, L_2, L_3 - Lenses, S - Sample. BS - Beam splitter, F - Neutral density filter, PD - Photodiode, θ - angle at which the scattered light was collected.

field. The scattering is clearly visible for the 532 nm excitation, whereas at 435 nm, we have not observed such scattering as the lower input fluences are used. However, the observed nonlinear-scattered fluences are much lower ($<500\ \mu J\ cm^{-2}$) and are neglected while evaluating the parameters leading to optical limiting.

Nonlinear transmittance and scattering experiments are carried out using the f/30 geometry. The nonlinear transmittance is collected on-axis and the nonlinear scattering is collected at different angles from the axis. The experimental setup is shown in Fig 6. The nonlinear transmittance collected on-axis (○○○) and the scattering (×××) at an angle of 3.3° from the axis are shown in Fig. 7. At a higher fluence, the increase in the scattering and a corresponding decrease in the on-axis transmittance can be clearly seen. The scattered intensity shown in Fig. 7 is scaled in arbitrary units for comparison. We have observed a reduction in the scattering energy, with an increasing angle from the beam axis. Figure 8(a) shows the scattering at angles of 3.3° and 10° from the *Z* axis for the 1Ag1Cu film and Fig. 8(b) at 3.3° for the 1Ag2Cu and 1Ag3Cu films. The observed scattering has also reduced with the decreasing average particle size from 1Ag1Cu film to 1Ag3Cu film. At a lower fluence, though the amplitude of scattering is less, we have observed a nonlinear absorption. The nonlinear scattering in nanoparticles is reported to be due to the photoinduced mismatch of the medium,[36] i.e., the difference in the refractive indices of Ag and Cu nanoparticles with the silica film and the size of the nanoparticles. Size effects are reported in the case of Au nanoparticle systems,[32] where the OL effects are observed at lower intensities for ~15 nm size particles, whereas smaller particles of ~2 nm do not show any limiting effects. We have observed a surface damage at the fluence around 75 J cm^{-2}, where the transmission has reduced drastically and the films underwent an irreversible damage. The observed scattering is therefore due to the metal nanoparticles and not due to the damage to the film. Sol-gel films are well known to remain stable up to a very high fluence of as high as 300 J cm^{-1} in the nanosecond regime.[37] Though the nonlinear scattering has decreased with a decreasing particle size from 1Ag1Cu (40–50 nm) to 1Ag3Cu (15–20 nm), the nonlinear absorption has increased with a reducing particle size (i.e., increasing copper concentration). This is due to the fact that the excitation wavelength is closer to the surface-plasmon resonance of Cu nanoclusters.

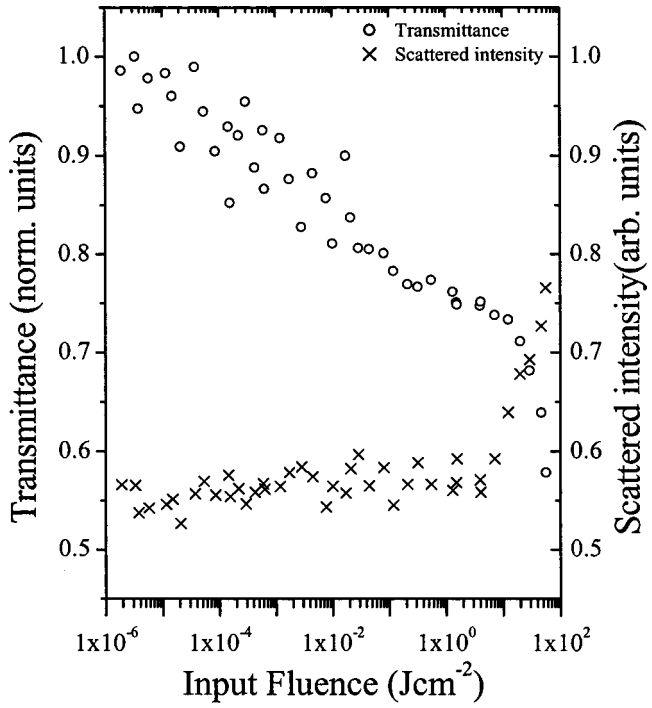

FIG. 7. Nonlinear transmittance (○) and scattering (×) for the 1Ag2Cu sol-gel film. The nonlinear scattering is scaled for comparison.

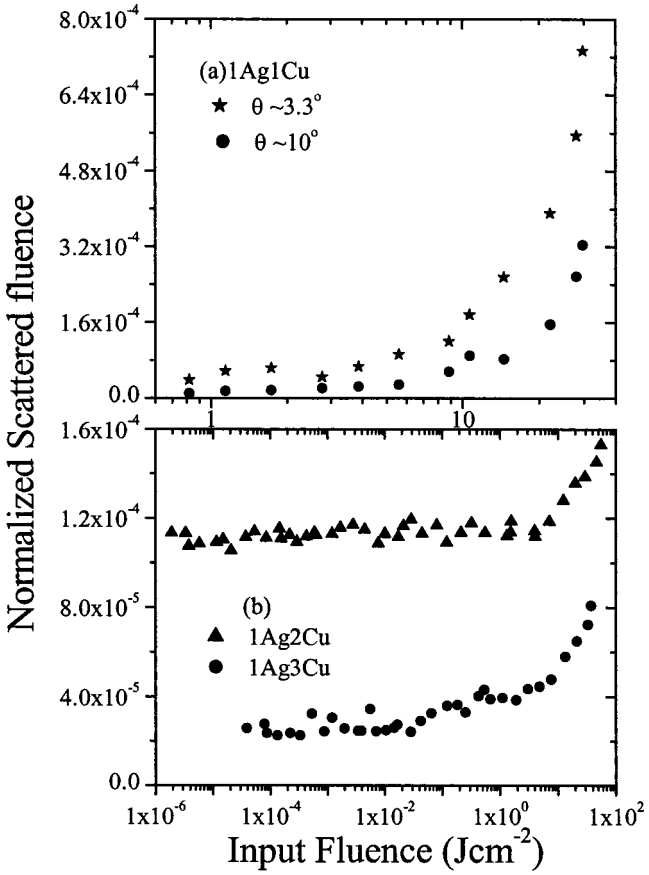

FIG. 8. Scattering curves (a) at $\theta \sim 3.3°$ and 10° for 1Ag1Cu film, (b) at 3.3° for 1Ag2Cu and 1Ag3Cu films for $\lambda_{ex} \sim 532$ nm.

To conclude, we have studied the nonlinear optical properties of SiO_2 films co-doped with Ag–Cu nanoclusters using the sol-gel method. These films show self-defocusing nonlinearities in both the nanosecond and picosecond regime and a good nonlinear absorption leading to the OL behavior in the nanosecond regime. The OL properties of Ag–Cu co-doped nanoclusters are investigated at three different wavelengths to understand the contribution of SPR toward it.

ACKNOWLEDGMENTS

The authors acknowledge the financial support from DRDO and DAE-BRNS, India. One of the authors (G. D.) thanks the Director, CGCRI, for the permission to carry out this work and DST, Government of India for the financial support. One of the authors (P.P.K.) also thanks CSIR, India, for Senior Research Fellowship. The authors thank Professor Deepak Mathur for extending the 25 ps laser facility.

[1]U. Kreibig and M. Vollmer, *Optical properties of metal clusters* (Springer, Berlin, 1995).
[2]Y. P. Sun, J. E. Riggs, K. B. Henbest, and R. B. Martin, J. Nonlinear Opt. Phys. Mater. **9**, 481 (2000).
[3]D. Ricard, Ph. Roussignol, and C. Flytzanis, Opt. Lett. **10**, 511 (1985).
[4]L. Yang, *et al.*, J. Opt. Soc. Am. B **11**, 457 (1994).
[5]T. Tokizaki, A. Nakamura, S. Kaneko, K. Uchida. S. Omi, H. Tanji, and Y. Asahara, Appl. Phys. Lett. **65**, 941 (1994).
[6]Y. Hamanaka, A. Nakamura, S. Omi, N. Del Fatti, F. Vallee, and C. Flytzanis, Appl. Phys. Lett. **75**, 1712 (1999).
[7]N. Del Fatti and F. Vallee, Appl. Phys. B: Lasers Opt. **73**, 383 (2001).
[8]*Optical Power Limiting*, Proceedings of the Second International Symposium [ISOPL 2000], Venice, Italy, 2–5 July 2000, edited by R. Bozio and F. Kajzar.
[9]L. W. Tutt and T. F. Boggess, Prog. Quantum Electron. **17**, 299 (1993).
[10]Q. F. Zhang, W. M. Li, Z. Q. Xue, J. L. Wu, S. Wang, D. L. Wang, and Q. H. Gong, Appl. Phys. Lett. **82**, 958 (2003).
[11]J. Olivares, *et al.*, J. Appl. Phys. **90**, 1064 (2001).
[12]R. Philip, G. Ravindra Kumar, N. Sandhyarani, and T. Pradeep, Phys. Rev. B **62**, 13160 (2000).
[13]S. Qu, *et al.*, Opt. Commun. **203**, 283 (2002).
[14]M. R. V. Sahyun, S. E. Hill, N. Serpone, R. Danesh, and D. K. Sharma, J. Appl. Phys. **79**, 8030 (1996).
[15]K. Uchida, *et al.*, J. Opt. Soc. Am. B **11**, 1236 (1994).
[16]M. Falconieri, *et al.*, Appl. Phys. Lett. **73**, 288 (1998).
[17]G. De, J. Sol-Gel Sci. Technol. **11**, 289 (1998).
[18]N. Sanz, A. Ibanez, Y. Morel, and P. L. Baldeck, Appl. Phys. Lett. **78**, 2569 (2001).
[19]K. V. Yumashev, N. N. Posnov, I. A. Denisov, P. V. Prokoshin, V. P. Mikhailov, V. S. Gurin, V. B. Prokopenko, and A. A. Alexeeno, J. Opt. Soc. Am. B **17**, 572 (2000).
[20]N. Sanz, P. L. Baldeck, and A. Ibanez, Synth. Met. **115**, 229 (2000).
[21]M. Meneghetti, *et al.*, Synth. Met. **103**, 2474 (1999).
[22]G. De, L. Tapfer, M. Catalano, G. Battaglin, F. Caccavale, F. Gonella, P. Mazzoldi, and R. F. Haglund, Jr., Appl. Phys. Lett. **68**, 3820 (1996).
[23]G. De, G. Mattei, P. Mazzoldi, C. Sada, G. Battaglin, and A. Quaranta, Chem. Mater. **12**, 2157 (2000).
[24]S. Link, C. Burda, Z. L. Wang, and M. A. El-Sayed, J. Chem. Phys. **111**, 1255 (1999).
[25]M. Sheik-Bahae, A. A. Said, T. H. Wei, D. J. Hagan, and E. W. Van Stryland, IEEE J. Quantum Electron. **26**, 760 (1990).
[26]R. F. Haglund, Jr., L. Yang, R. H. Magruder, III, J. E. Witting, K. Becker, and R. A. Zuhr, Opt. Lett. **18**, 373 (1993).
[27]J. M. Ballesteros, J. Sollis, R. Serna, and C. N. Afonso, Appl. Phys. Lett. **74**, 2791 (1999).
[28]D. H. Osborne, Jr., R. F. Haglund, Jr., F. Gonella, and F. Garrido, Appl. Phys. B: Lasers Opt. **66**, 517 (1998).
[29]R. W. Boyd, *Nonlinear Optics* (Academic, San Diego, CA, 1992), Chap. 4.
[30]P. Mazzoldi, G. W. Arnold, G. Battaglin, F. Gonella, and R. F. Huglund, Jr., J. Nonlinear Opt. Phys. Mater. **5**, 285 (1996).
[31]P. V. Kamat, M. Flumiani, and G. V. Hartland, J. Phys. Chem. B **102**, 3123 (1998).
[32]L. Francois, M. Mostafavi, J. Belloni, J. F. Delouis, J. Delaire, and P. Feneyrou, J. Phys. Chem. B **104**, 6133 (2000).
[33]J.-Y. Bigot, V. Halte, J.-C. Merle, and A. Daunois, Chem. Phys. **251**, 181 (2000).
[34]N. Del Fatti, F. Vallee, C. Flytzanis, Y. Hamanaka, and A. Nakamura, Chem. Phys. **251**, 215 (2000).
[35]V. Halte, J.-Y. Bigot, B. Palpant, M. Broyer, B. Prevel, and A. Perez, Appl. Phys. Lett. **75**, 3799 (1999).
[36]V. Joudrier, P. Bourdon, F. Hache, and C. Flyzanis, Appl. Phys. B: Lasers Opt. **67**, 627 (1998).
[37]L. Smilowitz, *et al.*, Synth. Met. **84**, 931 (1997).